Manuscript prepared for Earth Syst. Dynam. Discuss.
with version 4.1 of the LaTeX class copernicus_discussions.cls.
Date: 25 August 2014

Explaining the seasonal cycle of the globally averaged CO_2 with a carbon cycle model

G.A. Alexandrov

A.M. Obukhov Institute of Atmospheric Physics, Russian Academy of Sciences, Pyzhevsky 3, Moscow, 119017

Correspondence to: G.A. Alexandrov
(g.alexandrov@ifaran.ru)

Abstract

The seasonal changes in the globally averaged atmospheric carbon dioxide concentrations reflect an important aspect of the global carbon cycle: the gas exchange between the atmosphere and terrestrial biosphere. The data on the globally averaged atmospheric carbon dioxide concentrations which are reported by NOAA/ESRL could be used to demonstrate the adequacy of the global carbon cycle models. However, it was found recently that the observed amplitude of seasonal variations in the atmospheric carbon dioxide concentrations is higher than simulated. In this paper, the factors that affect the amplitude of seasonal variations are explored using a carbon cycle model of reduced complexity. The model runs show that the low amplitude of the simulated seasonal variations may result from underestimated effect of substrate limitation on the seasonal pattern of heterotrophic respiration and from underestimated magnitude of the annual Gross Primary Production in the terrestrial ecosystems located to the north of 25N.

1 Introduction

The global mean monthly atmospheric concentrations of carbon dioxide provided by NOAA/ESRL (Conway and Tans, 2012) show that the carbon storage of the atmosphere undergoes regular seasonal changes. The amplitude of seasonal variations in the atmospheric carbon storage puts certain constraints on the choice of parameters in the models of global carbon cycle and the joint carbon-climate models. It would be natural to expect that models are tuned to reproduce the CO_2 growth curve – the basic scientific evidence of the global change, but this not the case. One may find papers demonstrating that carbon cycle models coupled with atmospheric transport models could reproduce seasonal cycle of CO_2 concentrations at some locations (Heimann et al., 1998; Dargaville et al., 2002; Randerson et al., 2009; Cadule et al., 2010; Anav et al. , 2013). However, it is difficult to find an article comparing simulated seasonal variations in the atmospheric carbon storage with the globally averaged monthly concentrations of carbon dioxide reported by NOAA/ESRL. A recent article (Chen, 2011) reporting the results of such comparison brings bad news: the observed amplitude of seasonal variations in the atmospheric

carbon storage is larger than simulated. Where does the discrepancy come from? According to Chen (2011), "The apparent discrepancy between modeling results and observations results from the "representation error" of observation stations" (Chen, 2011). This assumption is challenged here by demonstrating that the discrepancy can be reconciled through model tuning.

2 Methods

2.1 Net carbon exchange between the atmosphere and other pools

2.1.1 Observations

The seasonal cycle of the atmospheric carbon storage reflects the seasonal cycle of the net carbon exchange between the atmosphere and other pools. The de-trended net exchange (N_a) is derived from the de-trended atmospheric carbon storage (dC_a), which in its turn is calculated from the de-trended globally averaged monthly concentrations of carbon dioxide in the atmosphere ($d[CO_2]$) reported by NOAA/ESRL (Conway and Tans, 2012): $dC_a(m) = 2.13 \times d[CO_2](m)$. Since $dC_a(m)$ is the value of dC_a in the middle of the month m, the value of dC_a in the beginning of the month m is calculated as the mean of its values in the middle of this month and in the middle of the preceding month, that is, as $(dC_a(m-1)+dC_a(m))/2$, and the value of dC_a in the end of the month m is calculated as the mean of its values in the middle of this month and in the middle of the following month, that is, as $(dC_a(m)+dC_a(m+1))/2$. Then $N_a(m)$ is calculated as the difference between the value of dC_a in the end of the month m and its value in the beginning of the month m :

$$N_a(m) = \frac{dC_a(m)+dC_a(m+1)}{2} - \frac{dC_a(m-1)+dC_a(m)}{2} \tag{1}$$

that gives

$$N_a(m) = \frac{dC_a(m+1)-dC_a(m-1)}{2}. \tag{2}$$

The accuracy of monthly N_a estimates is determined by the accuracy of monthly $d[CO_2]$ estimates. Since monthly $d[CO_2]$ estimates are derived from local observations (Masarie and Tans, 1995), the accuracy of monthly N_a estimates depends on the adequacy of the observation network (Appendix 2).

2.1.2 Modelling

The monthly N_a estimates could be also calculated using the following equation:

$$N_a(m) = -GPP(m) + R_a(m) + R_h(m) + \nu_a(m) \tag{3}$$

where GPP, R_a, and R_h are gross primary production, autotrophic respiration, and heterotrophic respiration of the terrestrial ecosystems, and ν_a is net carbon exchange between the atmosphere and remaining carbon pools.

The seasonal cycle of GPP, R_a, and R_h is simulated here using the concepts of the MONTHLYC model (Box, 1988) and the global fields of monthly actual evapotranspiration (Willmott, 1985) and monthly air temperature (Leemans and Cramer, 1991) gridded at a 0.5 x 0.5 degree resolution.

The seasonal cycle of GPP is determined in the MONTHLYC model by the monthly actual evapotranspiration, $AET(m)$:

$$GPP(m) = \frac{AET(m)}{\sum_{m=1}^{12} AET(m)} GPP_{ann} \tag{4}$$

where GPP_{ann}, the annual GPP, is derived from the Montreal NPP model.

The Montreal NPP model relates annual net primary production (NPP_{ann}, in $gC\ m^{-2}\ yr^{-1}$) to annual actual evapotranspiration (AET_{ann}, in $mm\ yr^{-1}$) (Box, 1988):

$$NPP_{ann} = 1350 \cdot (1 - e^{-0.0009695 \cdot (AET_{ann} - 20)}) \tag{5}$$

and GPP_{ann} is derived from NPP_{ann} using the empirical equation (Box, 1988)

$$GPP_{ann} = -1863 \cdot \ln(1 - NPP_{ann}/1350) \tag{6}$$

that gives

$$GPP_{ann} = 1.8062 \cdot (AET_{ann} - 20) \tag{7}$$

where 1.8062 is the value characterising the water-use efficiency, WUE, the amount of GPP in gC produced per 1 liter of the water transpired. Hence, the general form of this equation is as follows:

$$GPP_{ann} = WUE \cdot (AET_{ann} - 20) \tag{8}$$

The monthly values of R_a in the MONTHLYC model are proportional to $Q_{10}^{\frac{T(m)-10}{10}}$ ($Q_{10} = 2$):

$$R_a(m) = \frac{Q_{10}^{\frac{T(m)-10}{10}}}{\sum_{m=1}^{12} Q_{10}^{\frac{T(m)-10}{10}}} R_{a,ann} \tag{9}$$

where $T(m)$ is monthly air temperature and $R_{a,ann}$ is the annual autotrophic respiration calculated as the difference between GPP_{ann} and NPP_{ann}:

$$R_{a,ann} = GPP_{ann} - NPP_{ann} \tag{10}$$

The monthly values of heterotrophic respiration from each litter pool depend in the MONTHLYC model on the rates of litter decay and the storage of litter:

$$R_{h,i}(m) = r_i(m)s_i(m) \tag{11}$$

where the monthly values of decay rates are proportional to monthly values of AET:

$$r_i(m) = \frac{AET(m)}{\sum_{m=1}^{12} AET(m)} r_{a,i} \tag{12}$$

and $r_{a,i}$ depends on the annual amount of AET (Box, 1988) as follows:

$$r_{a,i} = r0_{a,i} \cdot 10^{-1.4553+0.0014175 \cdot AET_{ann}} \tag{13}$$

The monthly values of litter storages satisfy in the MONTHLYC model the following difference equations:

$$s_i(m+1) = s_i(m) + p_i(m) - R_{h,i}(m) \tag{14}$$

where $p_i(m)$ is the input of organic matter to the i-th pool of litter. They are found by iterations.

Up till now all of the modelling formulation directly follows Box (1988). Modifications that I introduced to the MONTHLYC model were as follows.

Whereas Box (1988) used 3 litter pools: above-ground true litter (mostly leaves), root litter, and large woody debris (deadfall), I instead use two pools: the pool of slowly decaying fractions and the pool of quickly decaying fractions. The annual heterotrophic respiration is, thus, divided into heterotrophic respiration related to slowly decaying fractions of litter ($R_{h,s}$) and that related to quickly decaying fractions ($R_{h,q}$). The adequacy of this approach is discussed in the Appendix A1.

The seasonal changes in the storage of slowly decaying litter are small in comparison to its average value, and so the seasonal cycle of $R_{h,s}$ reflects that of the rate of decay, which is assumed to be proportional to $AET(m)$:

$$R_{h,s}(m) = \frac{AET(m)}{\sum_{m=1}^{12} AET(m)} R_{h,s,ann} \tag{15}$$

and

$$R_{h,s,ann} = (1-\phi) NPP_{ann} \tag{16}$$

where ϕ is the share of quickly decaying fractions in the litterfall, and $R_{h,s,ann}$ is the part of heterotrophic respiration related to slowly decaying fractions of litter, which in the case of de-trended carbon cycle is equal to the corresponding part of NPP_{ann}.

The storage of quickly decaying fractions is sensitive to the seasonal pattern of litterfall. Since deciduous trees shed leaves in the end of growing season, the part of heterotrophic respiration which is related to quickly decaying fractions may depend on the substrate availability. The seasonal changes in the storage of quickly decaying fractions of litter (s) are modelled here by the ordinary differential equation:

$$\frac{ds}{dt} = -r(t)s \tag{17}$$

where $r(t)$ is the rate of litter decay, and t is the time elapsed since the end of growing season. The function $r(t)$ is a periodical continuous function, $r(t+12) = r(t)$, the average value of which during the month m is proportional to monthly values of AET:

$$\int_{m-1}^{m} r(t)dt = \frac{AET(m)}{\sum_{m=1}^{12} AET(m)} \int_{0}^{12} r(t)dt \tag{18}$$

If litterfall occurs only in the end of growing season, then $s(0) = s(12) + p$, where p is equal to $\phi \cdot NPP_{ann}$. In this case,

$$s(n) = \frac{\phi \cdot NPP_{ann}}{1 - e^{-\int_0^{12} r(t)dt}} e^{-\int_0^{n} r(t)dt} \tag{19}$$

where n is the number of months elapsed since the end of growing season.

The storage of quickly decaying litter in a given month m is calculated using the equation

$$S(m, m_0) = \frac{\phi \cdot NPP_{ann}}{1 - e^{-\int_{m_0}^{m_0+12} r(t)dt}} e^{-\int_{m_0}^{m} r(t)dt} \tag{20}$$

where m_0 is the last month of the growing season and $m \geq m_0$. If $m < m_0$, then $S(m, m_0)$ is calculated as follows:

$$S(m; m_0) = \frac{\phi \cdot NPP_{ann}}{1 - e^{-\int_{m_0}^{m_0+12} r(t)dt}} e^{-\int_{m_0}^{m+12} r(t)dt} \tag{21}$$

Consequently, heterotrophic respiration related to decomposition of quickly decaying litter is calculated using the following equations:

$$R_{h,q}(m) = S(m-1; m_0) - S(m; m_0) \tag{22}$$

where the geographic distribution of m_0 is derived from the assumption that the growing season in the deciduous forests of Northern Hemisphere normally ends when monthly air temperature goes below 10°C (that is, in September or October), and that in some other ecoregions,

the end of growing season may occur due to the lack of precipitation, e.g., when monthly AET goes below 20 mm/month.

GPP, R_a, and R_h are the major drivers of the seasonal changes in the atmospheric carbon storage. The amplitude of seasonal changes in the carbon exchange between the atmosphere and the ocean is relatively small (e.g., Chen, 2011). The same can be said about the seasonal changes in the emissions from fossil fuels burning. Hence, one could assume that $N_{a,mod}(m) = -GPP(m) + R_a(m) + R_{h,s}(m) + R_{h,q}(m)$, may give a good approximation of $N_a(m)$ under some choice of ϕ, WUE and Q_{10} values. This assumption was tested by numerical experiments. The results are discussed below.

3 Results and Discussion

The global monthly GPP calculated using Eqs. (4-7) has a peak when N_a has a dip (Figs. 1-2), supporting the view that seasonal cycle of the globally averaged atmospheric CO_2 concentration reflects the seasonality of plant activity (Keeling et al., 1996). The effect of GPP is reduced, however, by autotrophic respiration (R_a) that has a peak at the same month as GPP. The part of the heterotrophic respiration that results from the decay of slowly decaying fraction of litter ($R_{h,s}$) also has a peak at the same month as GPP. Consequently, the amplitude of the seasonal changes in $N_{a,mod}$ could be very narrow if compared to that of N_a (Fig 3).

The discrepancy between the amplitude of the seasonal changes in $N_{a,mod}$ and that of N_a can be reconciled by increasing WUE, decreasing Q10 and increasing ϕ. The 'true' values of these model coefficients are not known, but they should fall within empirically established, or widely accepted, bounds. Jasechko et al. (2013) estimated the global WUE of the terrestrial biosphere to be 3.2 $\pm$ 0.9 mmol CO_2 per mol H_2O, that corresponds to the range from 1.5 to 2.7 gC per liter of water and suggests that 2.7 gC per liter of water can be taken as the highest possible estimate of WUE. Zhao and Running (2011) used 1.4 as the lowest possible estimate of Q10. The highest possible estimate of ϕ cannot exceed the share of herbaceous fractions in the litterfall, that varies from 0.3 in forests to 0.9 in grasslands (Esser, 1984). Parton et al. (1987) divided herbaceous litter into the pool of structural C, the residence time of which is 3

years, and the pool of metabolic C, the residence time of which is 0.5 year. Hence, the highest possible estimate of ϕ cannot exceed the share of herbaceous fractions in the litterfall multiplied by the share of metabolic C compounds in the herbaceous litter. The latter depends on lignin to nitrogen ratio, and thus could be very small in evergreen needleleaf forests. Moreover, Parton et al. (1987) assumed that only 55% of carbon are released to the atmosphere in course of fresh litter decomposition, whereas 45% go to the pools of soil organic matter. Thus, the possible values of ϕ could range from 0.1 to 0.3 depending on the share of land covered by grasslands and broadleaf forests. Numerical experiments show that the amplitude of the seasonal changes in $N_{a,mod}$ can be roughly of the same width as that of N_a under some values of WUE, Q10 and ϕ that fall within bounds mentioned above (Fig 4).

This result demonstrates that amplitude of the seasonal cycle of the globally averaged monthly concentrations of carbon dioxide reported by NOAA/ESRL could be simulated with a carbon cycle model. The simplicity of the model, which is used in this study, may raise doubts on its validity. Although the doubts of this sort are difficult to dispel due to the lack of standardized tools needed for adequate model evaluation (Alexandrov et al., 2011), the usage of the model could be legitimated as follows.

The purpose of the study is to understand behaviors of more complex models. Model complexity poses an obstacle for diagnosing the sources of discrepancy between model predictions and observations. Xia et al. (2013) show that one can overcome this obstacle by decomposing a complex model into traceable components. Another approach is to use minimal models, that is, the models of reduced complexity which are designed to explain only certain aspects of a system (Evans et al., 2013). Many aspects of complex model behaviors are beyond the scope of this study. Among them are the increasing amplitude of the seasonal changes in the globally averaged monthly concentrations of carbon dioxide (Graven et al., 2013) and the spatial distribution of soil carbon (Todd-Brown et al. , 2013). The version of the MONTHLYC model is used as a minimal model, that is, merely to explore the factors that affect the amplitude of seasonal changes in N_a.

One of these factors is substrate limitation that may be caused by the shift between the phase of NPP seasonal cycle and the seasonal cycle of litterfall production. The models and submodels

of litterfall production (e.g., Randerson et al., 1996; Potter et al., 1993; Box, 1988; Esser, 1987; Ito and Oikawa, 2002; Eliseev, 2011) often deal with such components as coarse woody debris, fine woody debris, leaf debris and so on. In this study all litter components were aggregated in two pools: slowly decaying fractions and quickly decaying fractions. The conceptual validity of this approach is explained in the Appendix A1.The pool of quickly decaying fractions is assumed to be refilled once per year (Fig 6) and depleted in summer. During the period of the pool depletion heterotrophs decomposing quickly decaying fractions become substrate-limited. This causes a decrease in monthly heterotrophic respiration below that expected from a model that does not take into account the effects of substrate availability. The decrease, which is referred to as substrate limitation (Randerson et al., 1996), depends on the share of quickly decaying fractions in the litterfall. Hence, the share of quickly decaying fractions in the litterfall is one of the parameters of the complex models of carbon cycle which are responsible for the amplitude of the simulated seasonal changes in N_a.

Another important factor is the annual magnitude of the terrestrial GPP. Beer et al. (2010) estimated it at 123$\pm$8 GtC/year. This estimate is close to the estimate that can be obtained with the MONTHLYC model for the original setting of WUE: Eq. (7) gives 129 GtC/year. If WUE is set at 2.7 gC/l, Eq.(8) gives 193 GtC/year. The highest possible estimate of the terrestrial GPP could be assessed using the Osnabruck collection of data on Net Primary Production (NPP) (Esser et al., 2000). The analysis of these data implies (Alexandrov et al., 1999) that the 90% confidence interval for the estimate of the terrestrial NPP is 52-81 GtC/year. Taking that GPP is often estimated by doubling NPP, one may conclude that the highest possible estimate of the terrestrial GPP should not exceed 160 GtC/year. The annual magnitude of the terrestrial GPP, perhaps, need not be set at 193 GtC/year in more complex models where WUE may vary depending on the vegetation type and the phase of the growing season.

The data on seasonal changes in NEE (Net Ecosystem Exchange) observed at Fluxnet sites (Falge et al. , 2005) allows us to see whether the model applied at the global scale can reproduce the seasonal cycle of local NEE. The results of simulations for the ”Hesse Forest” site (`HE99_dc_u0_mm.flx`), presented at the Figure 7, show that the model can reproduce the large part of the amplitude of the NEE seasonal cycle if the model coefficients are set at the

values that are used to reproduce the seasonal cycle of the globally averaged CO_2. At the same time, the Figure 7 shows that setting WUE at constant value over the whole year may underestimate GPP in the beginning of the growing season.

The results of the TransCom 3 experiment (Gurney et al., 2004) allows us to evaluate the ability of the model to reproduce the seasonal cycle of regional carbon fluxes. As can be seen from the Figure 8, setting WUE (and other model coefficients) at globally uniform value puts limitations on the domain of model application.

For Northern regions (Europe, Boreal North America, and Boreal Asia), the "green" version of the model (i.e., the version where WUE=2.7 gC/l, Q10=1.4, and $\phi = 0.2$) fits the results of the TransCom 3 experiment better than the "blue" version of the model (i.e., the version where WUE=1.8 gC/l, Q10=2.0, and $\phi = 0$) does. However, for South and North Africa, the "blue" version outperforms the "green" version. It also outperforms the "green" version for South America. As to the Tropical Asia, both green curve and blue curve fall within the wide range of uncertainty in TransCom's estimates, which is explained as follows: "Owing to limited CO_2 observations, tropical regions, particularly over land, show considerable uncertainty and may contain unrealistic seasonal swings in flux due to unconstrained adjustments to maintain the global mass balance constraint" (Gurney et al., 2004).

The model coefficients should be set on regional basis to reproduce the seasonal cycle of regional carbon fluxes. This is a conclusion that can be drawn from the Figure 8. However, it would be wrong to assume that setting model coefficients on regional basis would lead to dramatic changes in $N_{a,mod}$. The amplitude of seasonal changes in the total flux from Africa, South America, Tropical America, Tropical Asia, and Australia is much smaller than that of the total flux from Europe, non-tropical North America, and non-tropical Asia. There is no need to raise WUE of the tropical and Southern Hemisphere ecosystems. It can be kept at 1.8 gC/l. Since most seasonal changes in N_a can be attributed to seasonal changes in NEE in the ecosystems located to the north of 25N, the amplitude of $N_{a,mod}$ can be increased by raising WUE of these ecosystems.

The hypothesis that productivity of these ecosystems is currently underestimated and the hypothesis about the importance of substrate limitation are not mutually independent. The recent

studies on microbial priming of soil organic matter decomposition (Heimann and Reichstein, 2008; Luo et al., 2011; Qiao et al., 2014) reveal the link between productivity and substrate limitation: increase in quickly decaying litterfall accelerates decomposition of 'old' soil carbon.

Microbial priming of soil organic matter decomposition is one of the important mechanisms and processes that were not received proper attention in this study due to limitations of the MONTHLYC model. Hopefully, they will be addressed in further studies where more detailed models will be used to test working hypotheses proposed in this paper.

4 Conclusions

The amplitude of seasonal changes in the globally averaged atmospheric CO_2 concentrations characterizes an important aspect of the global carbon cycle. The fact that a complex carbon cycle model cannot reproduce it (Chen, 2011) raises the question about the adequacy of this and other models. Complexity makes it difficult to trace a model inadequacy back to its source. Therefore, the model which is used in this study omits many important details in sake of conceptual clarity. This allows us to reveal potential shortcomings. The low amplitude may result from underestimated annual magnitude of GPP in the terrestrial ecosystems located to the north of 25N and from underestimated effect of substrate limitation. The effect of substrate limitation could be lost if model structure does not include the pool of litterfall fractions which are decomposed within a year. Such deficiency can be corrected through modelling the seasonal pattern of the herbaceous litterfall and estimating the share of quickly decaying fractions in the herbaceous litterfall. As to the possible underestimation of GPP, this is a problem that cannot be resolved without re-analysis of all available data on GPP and NPP.

A1 Aggregation of litter pools

The model adequacy cannot be assessed without due regard to the context within which the model is used. The complexity of a detailed model can be significantly reduced if the model is applied to the ecosystem where the annual mean of the carbon stock in each carbon pool is

constant. The carbon flow through the pools can be represented as a stationary Markov chain in such case. The pools correspond to the states of the Markov chain. The probability of single-step transition from state j to state i is equal to

$$q_{ij} = \frac{f_{ij}}{\sum_{i=1}^{n} f_{ij}}$$

where f_{ij} is the carbon flow from the j-th pool to the i-th pool.

The average time that carbon which is residing in the j-th pool spends in the i-th pool before returning to the atmosphere is determined as follows (Logofet and Alexandrov , 1984):

$$t_{ij} = \frac{x_i}{\sum_{j=1}^{n} f_{ij}} \widetilde{q_{ij}}$$

where x_i is the steady-state carbon stock in the i-th pool, and $\widetilde{q_{ij}}$ is the element of the matrix $(\mathbf{I} - \mathbf{Q})^{-1}$, where $\mathbf{I}$ is the identity matrix and $\mathbf{Q} = (q_{ij})$.

The seasonal depletion of the carbon stock can be significant in the pool where

$$\frac{x_i}{\sum_{j=1}^{n} f_{ij}} < 1$$

if the sum of the all inputs to this pool undergoes severe seasonal changes. Such pools can be aggregated into a pool of quickly decaying organic matter, and the other pools can be aggregated into the pool of slowly decaying organic matter with little loss of accuracy.

For example, let us consider the Century model (Parton et al., 1987). The Century model incorporates 5 pools of carbon: metabolic C, structural C, active soil C, slow soil C, and passive soil C. The residence time of metabolic C is less than 0.5 year. The residence times of other pools are greater than 1.5 year (25 years in the case of slow soil C, and 1000 years in the case of passive soil C). Hence, significant seasonal depletion of carbon stock may occur only in the pool of metabolic C. Other pools may be aggregated into the pool of slowly decaying organic matter. The aggregation will have no effect on the seasonal changes in the heterotrophic respiration from these pools if the monthly rates of decay are proportional to monthly AET:

$$R_{h,s}(m) = \sum_{i=2}^{5} \frac{AET(m)}{\sum_{m=1}^{12} AET(m)} r_{a,i} s_i = \frac{AET(m)}{\sum_{m=1}^{12} AET(m)} \sum_{i=2}^{5} r_{a,i} s_i = \frac{AET(m)}{\sum_{m=1}^{12} AET(m)} r_{a,s} s_s$$

where

$$s_s = \sum_{i=2}^{5} s_i; r_{a,s} = \sum_{i=2}^{5} r_{a,i} \frac{s_i}{s_s}$$

A2 Is it reasonable to infer world monthly CO_2 fluxes from globally averaged monthly CO_2 concentrations?

Let us consider the two-box model that Engelen et al. (2002) used to exemplify some methodological issues of inverse modelling:

$$\frac{M}{2}\frac{dc_1}{dt} = F_1 - \frac{M}{2}\kappa(c_1 - c_2)$$
$$\frac{M}{2}\frac{dc_2}{dt} = F_2 - \frac{M}{2}\kappa(c_2 - c_1)$$

where F_1 and F_2 are the net CO_2 fluxes, and c_1 and c_2 are average concentrations in the Northern and Southern Hemispheres, respectively, M is the coefficient that links the average CO_2 concentration and the CO_2 mass in the air column over a region, and κ is the exchange rate of air parcels between hemispheres.

Since

$$\frac{M}{2}\kappa(c_1 - c_2) + \frac{M}{2}\kappa(c_2 - c_1) = 0$$

this model implies

$$\frac{M}{2}\frac{dc_1}{dt} + \frac{M}{2}\frac{dc_2}{dt} = M\frac{d(\frac{c_1+c_2}{2})}{dt} = F_1 + F_2$$

and thus allows us to infer world monthly CO_2 fluxes, $F_1 + F_2$, from average monthly CO_2 concentrations in the Earth atmosphere, $(c_1 + c_2)/2$. The question is whether the globally averaged monthly concentrations of carbon dioxide reported by NOAA/ESRL provides an accurate estimate of the average monthly CO_2 concentrations in the Earth atmosphere.

To avoid answering this question one may first infer regional fluxes from the following system of the equations:

$$c_1 = h_{1,1}F_1 + h_{1,2}F_2 + ... + h_{1,n}F_n$$
$$c_2 = h_{2,1}F_1 + h_{2,2}F_2 + ... + h_{2,n}F_n$$
$$...$$
$$c_m = h_{m,1}F_1 + h_{m,2}F_2 + ... + h_{m,n}F_n$$

where m is the number of stations, n is the number of regions, c_i is CO_2 concentration observed at the i-th station ($i = 1, 2, ..., m$), F_j is CO_2 flux from the j-th region ($j = 1, 2, ..., n$), $h_{i,j}$ characterises the effect of the flux from j-th region on the CO_2 concentration at the i-th station.

And then, the world fluxes can be calculated as the sum of the regional fluxes.

The techniques for estimating coefficients $h_{i,j}$ and making inferences about regional fluxes are fairly complicated. One has to learn some fields of computational mathematics to understand how to do all necessary calculations. But will it give fluxes that will differ widely from those that could be inferred by using more simple technique?

At the Figure 9, the world monthly fluxes inferred from globally averaged monthly CO_2 concentrations are plotted against the results of TransCom 3 experiment (Gurney and Denning, 2013) presented in the form of box-and-whisker diagram. Twelve atmospheric transport models were used in this experiment to assess sensitivity of the flux estimates to the choice of transport model (Gurney et al., 2004). Besides, CASA model of net ecosystem production (Randerson et al., 1997) was used to keep the estimated fluxes within biogeochemically realistic bounds. The fluxes inferred from globally averaged monthly CO_2 concentrations (blue line) deviate significantly from the range of TransCom 3 estimates in June and November. Nevertheless the

shape of the blue line does not look strange: it seems that the world total monthly fluxes inferred from globally averaged monthly CO_2 concentrations fall within the range of accuracy of the atmospheric transport models and the techniques which are used for inversion of simulated tracer transport.

Acknowledgements. The research received financial support from the Russian Foundation for Basic Research, grant No 13-05-00781. The author also acknowledges intellectual support received from Alexey Eliseev, Nikolay Zavalishin, Maxim Arzhanov and Kirill Muryshev and highly appreciates the comments made by Ning Zeng and Ralph Keeling on earlier versions of this paper. The manuscript was thoroughly revised in response to the valuable comments of two anonymous reviewers who helped enormously to correct omissions.

References

Alexandrov, G.A., Ames, D., Bellocchi, G. et al.: Technical assessment and evaluation of environmental models and software: Letter to the editor. Environmental Modelling and Software, 26 (3), 328-336, 2011.

Alexandrov, G.A., Oikawa, T. and Esser, G.: Estimating terrestrial NPP: what the data say and how they may be interpreted? Ecological Modelling, 117, 361–369, 1999.

Anav, A., Friedlingstein, P., Kidston, M. et al.: Evaluating the Land and Ocean Components of the Global Carbon Cycle in the CMIP5 Earth System Models. Journal of Climate. 26, 6801–6843, 2013.

Beer, C., Reichstein, M., Tomelleri, E. et al.: Terrestrial Gross Carbon Dioxide Uptake: Global Distribution and Covariation with Climate. Science, 329, 834-838, 2010.

Box, E.O.: Estimating the seasonal carbon source-sink geography of a natural steady-state terrestrial biosphere. J. Appl. Meteorology, 27, 1009-1124, 1998.

Cadule, P., Friedlingstein, P., Bopp, L. et al.: Benchmarking coupled climate-carbon models against longterm atmospheric CO2 measurements. Global Biogeochemical Cycles, 24, GB2016, 2010.

Chen, Z-H.: Impacts of Seasonal Fossil and Ocean Emissions on the Seasonal Cycle of Atmospheric CO_2. Atmospheric and Oceanic Science Letters, 2011, 4: 70-74, 2011.

Conway, T.J. and Tans, P.: Recent Global CO_2, http://www.esrl.noaa.gov/gmd/ccgg/trends/global.html, 2012.

Dargaville, R.J., Heimann, M., McGuire, A.D. et al.: Evaluation of terrestrial carbon cycle models with atmospheric CO2 measurements: results from transient simulations considering increasing CO_2, climate, and land-use effects. Global Biogeochemical Cycles, 16, 1092-, 2002.

Eliseev, A.V.: Estimation of changes in characteristics of the climate and carbon cycle in the 21st century accounting for the uncertainty of terrestrial biota parameter values. Izvestiya Atmospheric and Oceanic Physics, 47, 131-153, 2011.

Engelen, R.J., Denning, A.S. and Gurney, K.R.: On error estimation in atmospheric CO2 inversions. Journal of Geophysical Research: Atmospheres, 107, ACL 10-1 – ACL 10-13, 2002.

Esser, G.: The significance of biospheric carbon pools and fluxes for the atmospheric CO2: A proposed model structure. Progress in Biometeorology, 3, 253–294, 1984.

Esser, G.: Sensitivity of global carbon pools and fluxes to human and potential climatic impacts. Tellus B, 39B, 245–260, 1987.

Esser, G., Lieth, H.F.H., Scurlock, J.M.O., and Olson, R.J.: Osnabrück net primary productivity data set. Ecology, 81, 1177-, 2000.

Evans, M.R., Grimm, V., Johst, K. et al.: Do simple models lead to generality in ecology? Trends in Ecology and Evolution, 28, 578 - 583, 2013.

Heimann, M., Esser, G., Haxeltine, A. et al.: Evaluation of terrestrial carbon cycle models through simulations of the seasonal cycle of atmospheric CO_2: first results of a model inter-comparison study. Global Biogeochemical Cycles, 12, 1–24, 1998.

Heimann, M. and Reichstein, M.: Terrestrial ecosystem carbon dynamics and climate feedbacks. Nature, 451, 289-292, 2008.

Falge, E., Aubinet, M., Bakwin, P. et al.: FLUXNET Marconi Conference Gap-Filled Flux and Meteorology Data, 1992-2000. Data set. Available on-line [http//www.daac.ornl.gov] from Oak Ridge National Laboratory Distributed Active Archive Center, Oak Ridge, Tennessee, U.S.A., 2005.

Graven, H.D., Keeling, R.F., Piper, S.C. et al.: Enhanced Seasonal Exchange of CO2 by Northern Ecosystems Since 1960. Science, 341, 1085-1089, 2013.

Gurney, K.R., Law, R.M., Denning, A.S. et al.: Transcom 3 inversion intercomparison: Model mean results for the estimation of seasonal carbon sources and sinks. Global Biogeochemical Cycles, 18, GB1010, doi:10.1029/2003GB002111, 2004.

Gurney, K.R. and Denning, A.S.: TransCom 3: Seasonal CO2 Flux Estimates from Atmospheric Inversions (Level 2). Data set. Available on-line [http://daac.ornl.gov/] from Oak Ridge National Laboratory Distributed Active Archive Center, Oak Ridge, Tennessee, USA. doi:10.3334/ORNLDAAC/1198

Jasechko, S., Sharp, Z. D., Gibson, J. J. et al.: Terrestrial water fluxes dominated by transpiration. Nature, 496, 347-350.

Ito, A. and Oikawa, T.: A simulation model of the carbon cycle in land ecosystems (Sim-CYCLE): a description based on dry-matter production theory and plot-scale validation. Ecological Modelling, 151, 143-176, 2002.

Keeling, C.D., Chin, J.F.S. and Whorf, T.P.: Increased activity of northern vegetation inferred from CO_2 measurements, Nature, 382, 146-149,1996.

Leemans, R. and Cramer, W.: The IIASA database for mean monthly values of temperature, precipitation, and cloudiness on a global terrestrial grid, IIASA Research Report RR-91-18, 1991.

Logofet, D.O. and Alexandrov, G.A.: Modelling of matter cycle in a mesotrophic bog ecosystem I. Linear analysis of carbon environs. Ecological modelling 21 (4), 247-258, 1984.

Luo Y.,Durenkamp M., De Nobili M. et al.: Short term soil priming effects and the mineralisation of biochar following its incorporation to soils of different pH. Soil Biol. Biochem. 43, 2304–2314, 2011.

Masarie, K.A., and Tans, P.: Extension and integration of atmospheric carbon dioxide data into a globally consistent measurement record, J Geophys Research, 100, 11593-11610, 1995.

Nassar, R.,Jones, D.B.A., Suntharalingam, P. et al.: Modeling global atmospheric CO2 with improved emission inventories and CO2 production from the oxidation of other carbon species, Geosci. Model Dev., 3, 689-716, 2010.

Parton, W.J., Schimel, D.S., Cole, C.V., and Ojima, D.S.: Analysis of factors controlling soil organic matter levels in Great Plains grasslands. Soil Sci. Soc. Am. J., 51, 1173-1179, 1987.

Potter, C. S., Randerson, J.T., Field, C. B., Matson, P. A., Vitousek, P. M., Mooney, H. A., Klooster, S. A.: Terrestrial ecosystem production: a process model based on global satellite and surface data. Global Biogeochemical Cycles, 7, 811-841, 1993.

Qiao, N., Schaefer, D., Blagodatskaya, E. et al.: The specific effects by priming of SOC depend on the amount and frequency of C inputs. Glob Chang Biol., 20, 1943-1954, 2014.

Randerson, J. T., Thompson, M. V. , Malmstrom, C. M., Field, C. B. and Fung, I. Y.: Substrate limitations for heterotrophs: Implications for models that estimate the seasonal cycle of atmospheric CO2. Global Biogeochemical Cycles, 10, 585–602,1996.

Randerson, J. T., Thompson, M. V. , Conway, T.J. et al.: The contribution of terrestrial sources and sinks to trends in the seasonal cycle of atmospheric carbon dioxide, Global Biogeochem. Cycles, 11, 535–560,1997.

Randerson, J. T., Hoffman, F. M., Thornton, et al.: Systematic assessment of terrestrial biogeochemistry in coupled climate–carbon models. Global Change Biology, 15, 2462–2484, 2009.

Todd-Brown, K., Randerson, J.T., Post, et al.: Causes of variation in soil carbon simulations from CMIP5 Earth system models and comparison with observations, Biogeosciences, 10, 1717–1736, 2013.

Zhao, M. and Running, S.W.: Response to Comments on "Drought-Induced Reduction in Global Terrestrial Net Primary Production from 2000 Through 2009". Science, 333, 1093-1093, 2011.

Willmott, C.J., Rowe, C.M. and Mintz, Y.: Climatology of the terrestrial seasonal water cycle. J. Climatology, 5, 589-606, 1985.

Xia, J., Luo, Y., Wang, Y-P. and Hararuk, O.: Traceable components of terrestrial carbon storage capacity in biogeochemical models. Global Change Biology, 19, 2104-2116, 2013.

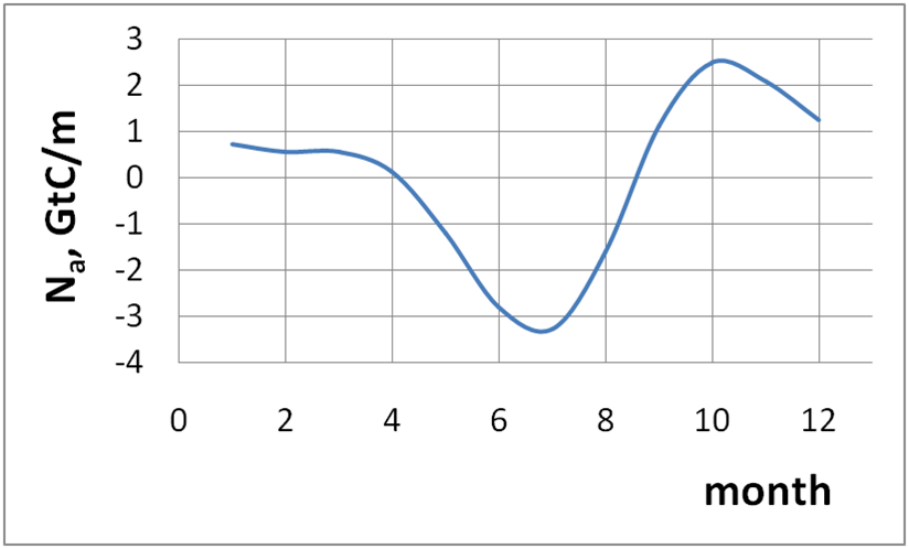

Fig. 1. Seasonal cycle of the de-trended net carbon exchange between the atmosphere and other pools (N_a) in 1995-2005.

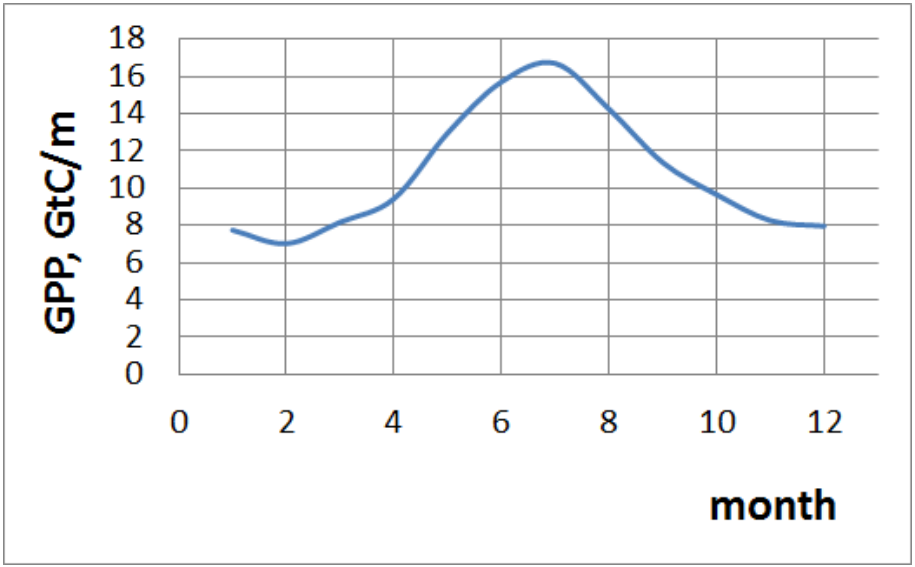

Fig. 2. Seasonal cycle of the Gross Primary Production (GPP) as calculated using Eqs. (4-7).

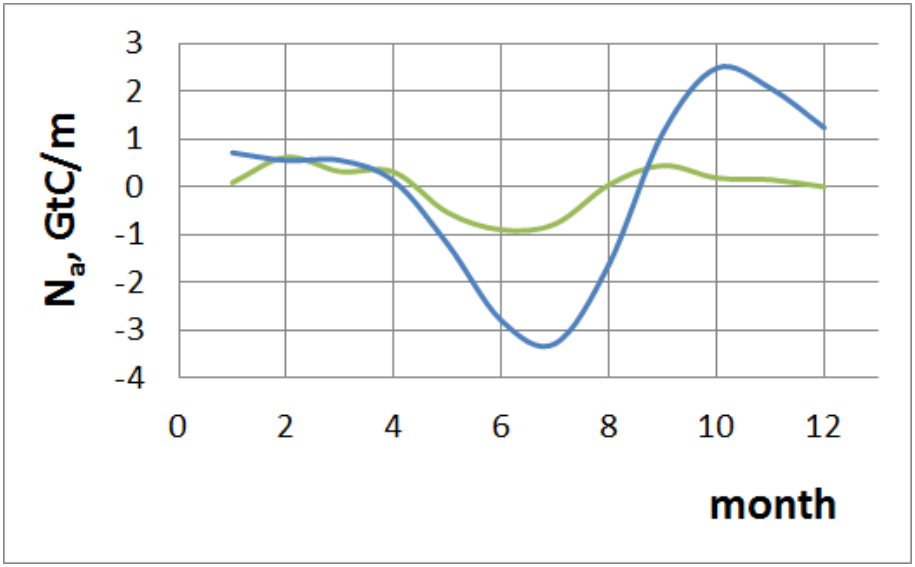

Fig. 3. The seasonal cycle of $N_{a,mod}$ (green) for WUE=1.8 gC/l, Q10=2.0, and $\phi = 0$, as compared to N_a (blue).

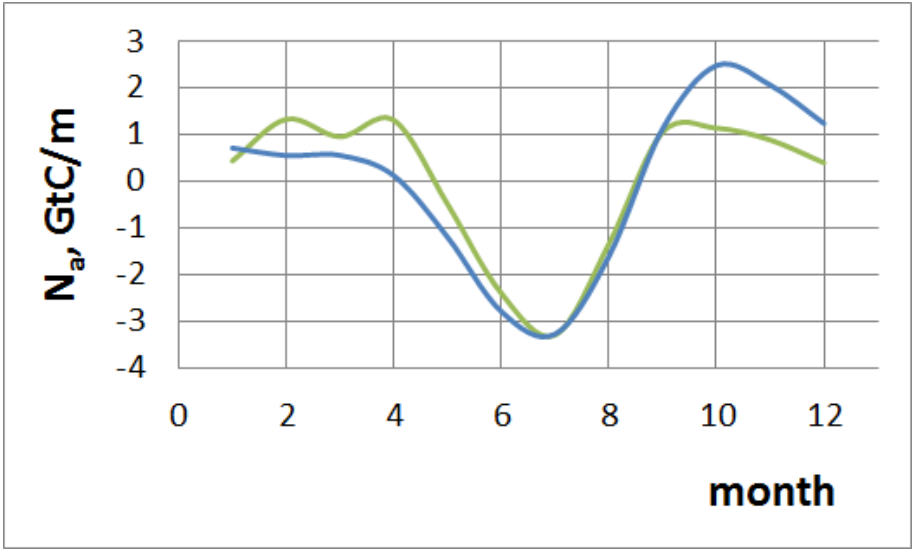

Fig. 4. The seasonal cycle of $N_{a,mod}$ (green) for WUE=2.7 gC/l, Q10=1.4, and $\phi = 0.2$, as compared to N_a (blue).

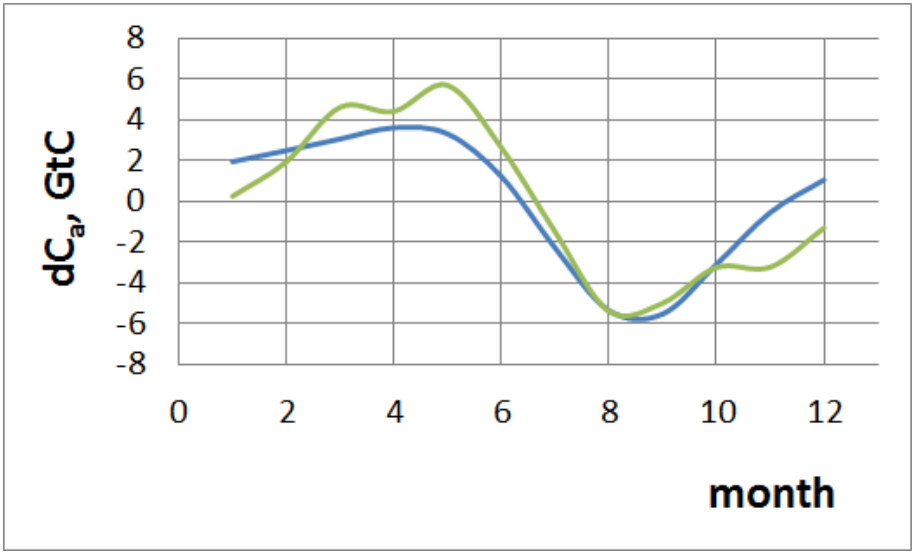

Fig. 5. The part of the seasonal cycle of the de-trended atmospheric carbon storage that could be attributed to the net exchange between the atmosphere and the terrestrial part of the biosphere (green) as compared to the total (blue).

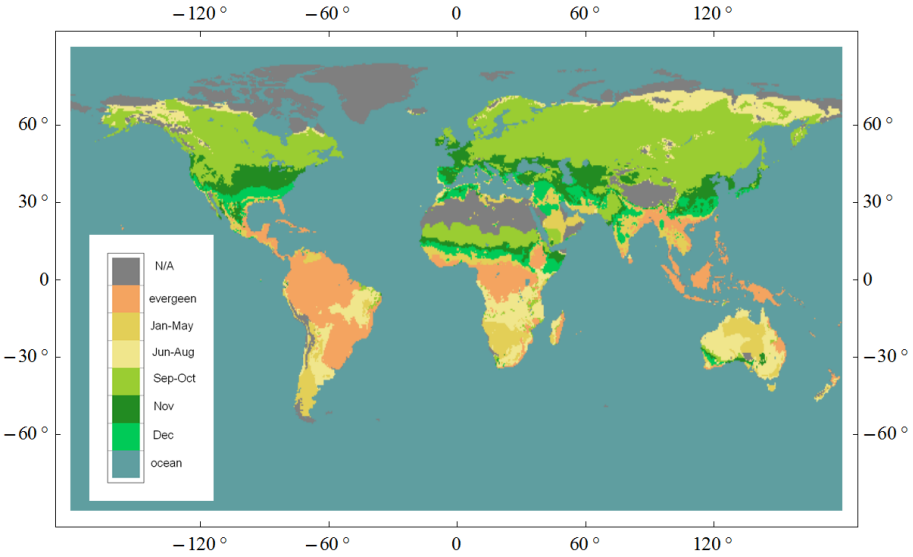

Fig. 6. The month at which deciduous trees supposedly shed leaves due to the end of growing season.

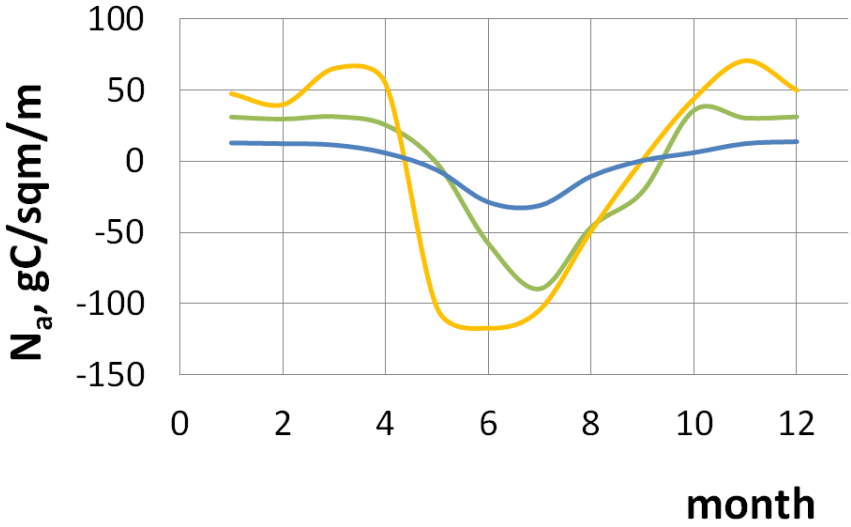

Fig. 7. The seasonal cycle of the local $N_{a,mod}$ for WUE=2.7 gC/l, Q10=1.4, and $\phi = 0.2$ (green) as compared that for WUE=1.8 gC/l, Q10=2.0, and $\phi = 0$ (blue) and to the observed de-trended NEE at the "Hesse Forest" site of Fluxnet (orange).

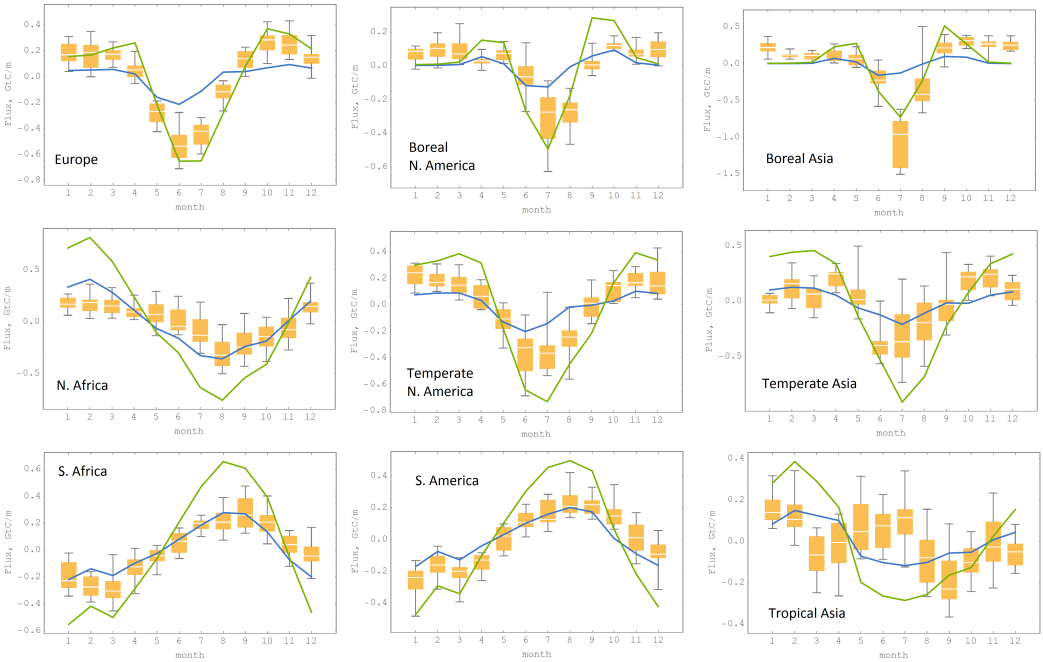

Fig. 8. The seasonal cycle of the regional $N_{a,mod}$ for WUE=2.7 gC/l, Q10=1.4, and $\phi = 0.2$ (green) as compared to that for WUE=1.8 gC/l, Q10=2.0, and $\phi = 0$ (blue), and to the de-trended TransCom 3 seasonal CO_2 flux (orange) estimated from atmospheric inversions (Gurney and Denning, 2013).

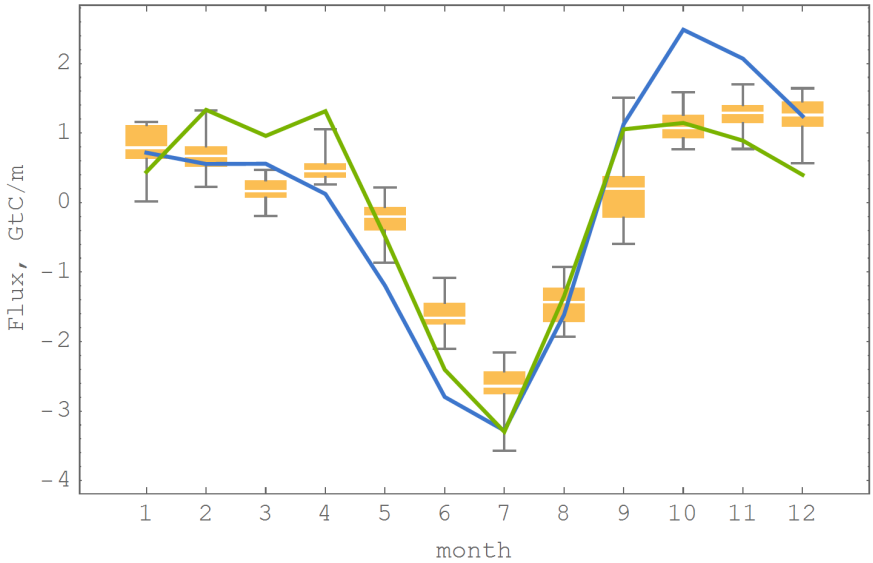

Fig. 9. The seasonal cycle of N_a (blue) as compared to the de-trended TransCom 3 seasonal CO_2 flux (orange) estimated from atmospheric inversions (Gurney and Denning, 2013). $N_{a,mod}$ for WUE=2.7 gC/l, Q10=1.4, and $\phi = 0.2$ is shown by the green line.